ISSN 0022-4766, Journal of Structural Chemistry, 2022, Vol. 63, No. 8, pp. 1291-1303. © Pleiades Publishing, Ltd., 2022.
Russian Text © The Author(s), 2022, published in Zhurnal Strukturnoi Khimii, 2022, Vol. 63, No. 8, 96300.

STRUCTURAL COMPLEXITY OF POLYMORPHS OF CALCIUM CARBONATE AND ITS CRYSTALLINE HYDRATES

D. A. Banaru[1], A. M. Banaru[2,3]*, and S. M. Aksenov[3]

The information content per contact in the net of contacts and in the critical net of structural units of $CaCO_3$ crystal modifications and $CaCO_3$ crystalline hydrates is calculated. Critical coordination numbers CN_{crit} and CN'_{crit} are determined by analysing the solid angles of Voronoi–Dirichlet polyhedra (VDPs) constructed for the center of mass of each structural unit. The following topological types are determined for all critical nets: **pcu** (primitive cubic packing) for calcite, postaragonite, **sra** ($SrAl_2$) for aragonite, **pts** (PtS) for vaterite, **qtz** (α- and β-quartz) for monohydrocalcite. In all structures, except for ikaite, the number of symmetrically independent contacts in the critical net coincides with its exact lower boundary. Thus, this rule of economy holds true not only in molecular crystals but also in other island structures.

DOI: 10.1134/S0022476622080108

Keywords: Voronoi–Dirichlet polyhedra, crystallographic net, calcium carbonate, information complexity.

INTRODUCTION

Calcium carbonate is one of the main components of carbonatites formed by a two-stage genesis from primary carbonate melts of Earth's mantle [1] and from sedimentary carbonate rocks. Carbonate minerals exhibit polymorphism, wide-range isomorphism, significant variations of the crystal order/disorder degree and are therefore very promising for the study of the geological past by structural crystallography methods [2]. Calcium carbonate occurs in nature as six crystal modifications: three anhydrous modifications (calcite, aragonite, vaterite) and two crystalline hydrates (monohydrocalcite $CaCO_3 \cdot H_2O$ and ikaite $CaCO_3 \cdot 6H_2O$) [3] which are dehydrated upon heating to thermodynamically stable calcite. Metastable two- and six-layer calcite polytypes were also predicted theoretically; as a result, assumptions about the mechanism of aragonite to calcite transformation were made [4]. Inorganic aragonite has some structural differences compared to biogenic aragonite [5]. Isostructural analogs of aragonite also include minerals strontianite $SrCO_3$, cerussite $PbCO_3$, and witherite $BaCO_3$ [6]. In contrast to calcite and aragonite, vaterite is metastable and forms polycrystalline spherulites with a diameter of 10-50 nm, which nevertheless may be essential for the biogenic calcification [6]. Ikaite is widespread in Arctic and Antarctic sea ice; according to the modern theories, it is produced there from organic substances and (partly) as a result of anaerobic methane oxidation [7]. Above 40 GPa, the structure of postaragonite (probably the most widespread carbon-containing

[1]Vernadsky Institute of Geochemistry and Analytical Chemistry, Russian Academy of Sciences, Moscow, Russia. [2]Lomonosov Moscow State University, Moscow, Russia; *banaru@phys.chem.msu.ru; banaru@mail.ru. [3]Kola Federal Research Center, Russian Academy of Sciences, Apatity, Russia. Original article submitted February 14, 2022; revised March 24, 2022; accepted March 25, 2022.

mineral in Earth's mantle) is stable; it was observed experimentally [8] and confirmed by theoretical predictions [9]. There are also other high-pressure $CaCO_3$ modifications [10-12] such as the theoretically predicted orthocarbonate structure Ca_2CO_4 [13], which is stable at 20-100 GPa and 1000-2000 K [14].

Disordered crystal structures of calcite [16] and aragonite [17] were determined more than half a century ago, while the ikaite structure was determined by XRD relatively recently [18]. The crystal structure of monohydrocalcite [19], which was solved in the $P3_1$ group by the Rietveld method using powder XRD data, complemented the earlier structural data on rotationally disordered carbonate ions with the $P3_121$ space group. The crystal structure of vaterite [20] was solved by direct methods using only precision electron diffraction data for nanocrystals with a linear size of ~50 nm. It is assumed that vaterite crystals, belonging to the same space group $C2/c$ as aragonite, undergo merohedral twinning to form fine powder characterized by a false hexagonal crystal system, thus explaining the fact why vaterite was initially assigned to the hexagonal system [6].

Borisov et al. in [15-17] and subsequent works published in JSC carried out a comprehensive crystallographic analysis of calcite, aragonite, and vaterite structures with atomic arrangements determined mainly by the relative positions of Ca^{2+} cations and the centers of mass of triangular CO_3 groups. The results of a similar analysis performed by the same authors for other series of minerals [18, 19] showed that atomic ordering during crystallization proceeds separately for anions and larger cations through different systems of crystallographic planes. The results of the analysis also suggest that the crystal structure's stability increases significantly with increasing rigidity of atomic localization by symmetry elements, i.e. for a smaller number of translational degrees of freedom. The relation between the stability and symmetry of the crystal structure was also discussed in the works by Shablovsky [20, 21].

If the contributions of enthalpy and entropy to the crystal's free energy are considered separately, the distribution of particles over crystallographic positions affects mainly the configurational entropy of the crystal [22]. The configuration entropy decreases with increasing diversity of occupied positions, but the information complexity of the crystal structure increases. According to Krivovichev [23], the structural information content per atom in a crystal is equal to

$$I_{\mathrm{G}}^{\mathrm{str}} = -\sum_{j=1}^{k} p_i \log_2 p_i (\text{bit/atom}), \tag{1}$$

$$p_i = m_i / v, \tag{2}$$

where m_i is the order of the ith occupied crystallographic orbit per reduced unit cell of the crystal; v is the total number of atoms in the reduced unit cell; k is the number of orbits occupied by atoms. The total information content per reduced unit cell is

$$I_{\mathrm{G,tot}}^{\mathrm{str}} = -v\sum_{j=1}^{k} p_i \log_2 p_i (\text{bit/u.c.}). \tag{3}$$

In the most general case, it can be expressed using the Shannon functional

$$H = \sum_{j=1}^{k} L(p_i), \tag{4}$$

where the information complexity of any chemical object, e.g. molecules [24] is estimated from

$$L(p_i) = \begin{cases} 0 (p_i = 0), \\ -p_i \log_2 p_i \quad (p_i > 0) \end{cases} \tag{5}$$

The set of orbits occupied by atoms in the crystal structure is determined by their interactions, but not vice versa, since in R. V. Galiulin's apt expression “atoms do not know space groups”. The strongest chemical bonds correspond to a particular set of symmetry operations generating a group [25-27], and this set is referred to as a fuzzy one due to the uncertainty in the choice of these bonds [28, 29]. After all, correctness of the Delone set for the points occupied by a crystal's structural units is determined by the local correctness of the system within a sphere of a finite radius [30, 31].

The set of generating contacts is usually distinguished from a large array of non-equivalent sets using the Voronoi–Dirichlet polyhedra (VDP) method (due to its simplicity) (Fig. 1) [32]. By means of their contacts, the structural units of a crystal form a 3D net which can be topologically analyzed and classified [33]. A combination of VDP and Monte Carlo

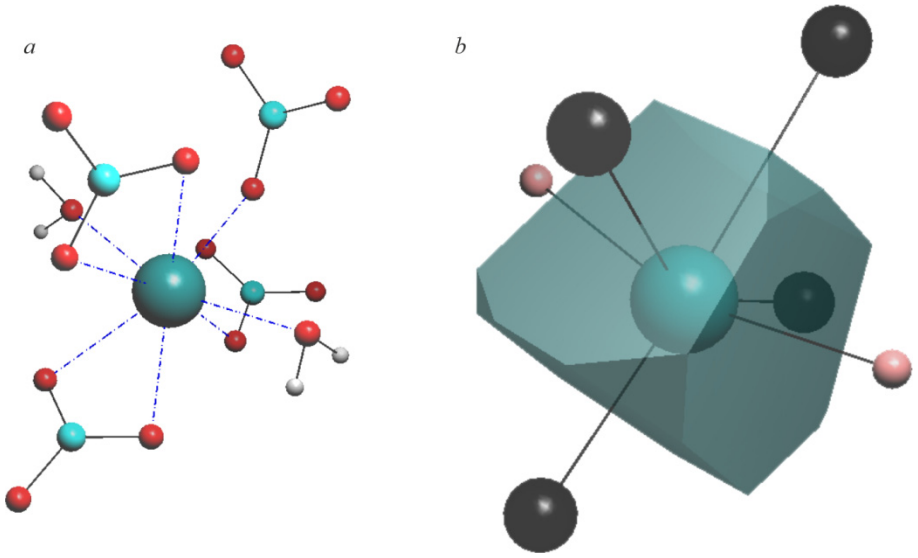

Fig. 1. First coordination sphere of $Ca^{2+(3)}$ (designations according to Table 3) in the structure of monohydrocalcite (*a*) and its VDP relative to the centers of mass of the ligands (*b*).

methods allows even predicting the crystal growth [34]. The analysis of nets simplified by the contraction of covalently bonded atoms to the center of mass of a system was conducted for the first time by Blatov and Zakutkin [35] on the example of anhydrous borates, nitrates, and carbonates, including calcite, aragonite, and vaterite; it was also noted that calcium carbonates are topologically similar to binary compounds NaCl and NiAs and that aragonite and vaterite constitute a "type–antitype" pair.

The procedure for identifying generating contacts using VDPs was initially applied to organic crystals [36-38]. In this work, generating contacts are identified for the first time in the crystal structure of minerals.

METHOD

In this work, only structural data without positional disorder were used. Since coordination numbers of structural units in a crystal are not very sensitive to the methods and conditions of determining atomic coordinates in the crystal structure, no other requirements were imposed on the crystal data in this work. The structural data were taken from the COD database [41] for aragonite [39], vaterite [40], monohydrocalcite [19], and ikaite [18]; from the AMCSD database [42] for calcite [16]; and from SpringerMaterials [46] for postaragonite [11].

The calculations were conducted using the ToposPro program [43]; the net classification was performed using RCSR [44] and topcryst [45] topological databases. The nets that are not classified in the databases were characterized by a point symbol [46]: notation $A^a.B^b\ldots$ means that a angles belonging to the shortest cycle A, b angles belonging to the cycle of the shortest cycle B, etc., converge at the vertex of the net, while $A < B < \ldots$ and $a + b + \ldots = CN(CN - 1)/2$.

The following algorithm was used to analyze the complexity of the studied crystal structures.

1. The adjacency matrix was constructed in each crystal structure from the VDPs of individual atoms by the domain method [47]. All non-covalent contacts, as well as all contacts with the participation of Ca^{2+} ions, were considered as net-forming ones (Fig. 2*a*).

2. Krivovichev's complexity [23] of a structure I_G^{str} (bit/atom) was calculated (in this work, it is denoted H_{comb}).

3. Each structural unit of a crystal was contracted to its center of mass while maintaining the adjacency between its structural units (Fig. 2*b*); the reduced unit cell of the resulting net contained v vertices (centers of mass) and e edges (contacts) occupying orbits v'' and e'', respectively. The assumed structural units in calcium carbonate polymorphs are Ca^{2+},

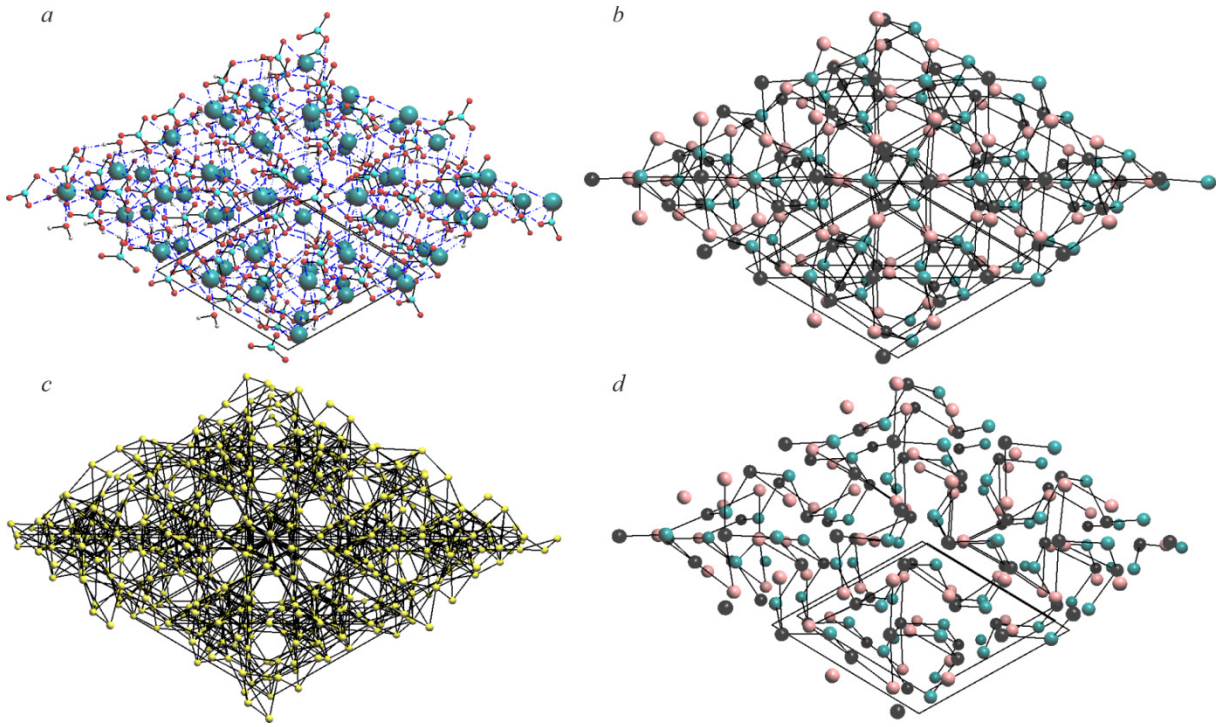

Fig. 2. Crystal structure of monohydrocalcite as projected along direction [001]: general form (*a*), centers of mass of adjacent structural units (*b*), edge net (*c*), critical net (*d*).

CO_3^{2-} groups, and water molecules (if present). If CN_i is the coordination number of the structural unit whose center of mass occupies the *i*th orbit in the crystal, then

$$\sum_{i=1}^{v''} v_i \cdot CN_i = 2e, \tag{7}$$

$$\sum_{i=1}^{v''} v_i = v. \tag{8}$$

The double prime is required to distinguish the number of net elements in the symmetrically independent part of the reduced unit cell (v' or e'), which can be fractional, in contrast to the number of occupied orbits.

4. Krivovichev's complexity for the centers of mass of structural units (H_{cm}, bit/center of mass) was calculated.

5. The edge net was constructed by replacing each edge by a vertex and each vertex by an edge (Fig. 2*c*). Two vertices of the edge net are adjacent to each other when and only when the corresponding edges in the original net come from the same vertex.

6. Complexity of the edge net [48] was calculated (bit/contact):

$$H_{edge} = -\sum_{j=1}^{e''} \frac{e_j}{e} \cdot \log_2 \frac{e_j}{e}, \tag{9}$$

where e_j is the number of edge net vertices occupying the *j*th orbit.

7. The net of generating contacts (critical net, Fig. 2*d*) was constructed in the descending order of solid angles Ω_j (in % of 4π steradian) for the VDPs of centers of mass of the structural units. All contacts with $\Omega_j < 0.5\%$ were removed from the original net, and the net of contacts was verified for being simply connected. If not, the original net was declared critical. If yes, all contacts with $\Omega_j < 1.0\%$ were removed, and the obtained net was verified for simple connectedness. If not, the previous net was declared critical. If yes, all contacts with $\Omega_j < 1.5\%$ were removed, etc. The procedure was repeated with a step of 0.5%, which approximately corresponds to the accuracy of solid angle calculations. The net that was not found simply connected at the next step was declared critical. The coordination number of the structural unit on the *i*th orbit of the

space group in the critical net is denoted $CN_{crit,i}$ when considering the symmetrically equivalent edges and $-CN'_{crit,i}$ (with a prime) otherwise. It is known [25] that the infimum of e'' in the critical net is calculated as

$$\inf(e''_{crit}) = |U_{SG}| + v'' - 1 - \sum_{i=1}^{v''} |U_{PG}|, \quad (10)$$

where U_{SG} is the minimum generating subset of the crystal's space group; U_{PG} is the minimal generating subset of the symmetry point group [49] of the molecule's position minus those elements which are not contained in any of the generating subsets of this space group (such elements are referred to as non-generating ones [29]); the parentheses denote the number of elements in the subset.

8. The edge net of the critical net was constructed and its complexity $H_{edge,crit}$ (bit/contact) was calculated.

9. Normalized values

$$SIC(H) = H / \max(H), \quad (11)$$

were calculated, where max(H) is the largest theoretically possible value of complexity H: $\max(H_{comb}) = \log_2 v$, $\max(H_{edge}) = \log_2 e$.

RESULTS AND DISCUSSION

The number of symmetrically independent formula units (Z'') is 1 in the crystal structures of calcite, aragonite and vaterite, 2 in ikaite, and 3 in monohydrocalcite. Table 1 lists the structural complexity values H_{comb} calculated for all atoms (a) and for the centers of mass of covalently bonded islands (b). Since only two orbits are occupied by the centers of mass of CO_3^{2-} and Ca^{2+} groups in calcite and aragonite structures, $H_{comb} = -1/2\log_2(1/2) - 1/2\log_2(1/2) = 1$ bit/center of mass; however, their complexity values per atom are different, since atoms occupy three orbits in calcite and four orbits in aragonite (H_{comb} = 1.371 bit/atom and 1.922 bit/atom, respectively). Both H_{comb} values and the corresponding SIC(H) values increase in the row from aragonite to vaterite, ikaite, and monohydrocalcite.

It has long been established that the calcite structure can be classified as a distorted NaCl structural type [50]; its topological type is **pcu**. Similarly, the aragonite and vaterite structures are classified as anti-NiAs and NiAs structural types, respectively [35]; their topological type is **nia**. Thus, in calcite, aragonite and vaterite, we have $CN(Ca^{2+} / CO_3^{2-}) = CN(CO_3^{2-} / Ca^{2+}) = 6$. The postaragonite structure belongs to the CsCl (**bcu**) type [11],

TABLE 1. Structural Data (space group (SG), occupied Wyckoff positions (WP)) and Structural Complexity of Ordered $CaCO_3$ Polymorphs

Structural data		Calcite	Aragonite	Postaragonite	Vaterite	Monohydrocalcite	Ikaite
SG		$R\bar{3}c$	$Pmcn$	$Pmmn$	$C2/c$	$P3_1$	$C2/c$
Z		6	4	2	12	9	4
Z''		1	1	1	2	3	1
Atoms	v	10	20	10	30	72	46
	v''	3	4	4	9	24	13
	WP	eba	dc^3	eba^2	f^6e^2c	a^{24}	$f^{10}e^3$
	H_{comb}, bit/atom	1.371	1.922	1.922	3.107	4.585	3.654
	SIC(H_{comb})	0.413	0.445	0.579	0.633	0.743	0.662
Centers of mass	v	4	8	4	12	27	16
	v''	2	2	2	4	9	5
	WP	ba	c^2	ba	f^2ec	a^9	f^3e^2
	H_{cm}, bit/center of mass	1.000	1.000	1.000	1.918	3.170	2.250
	SIC(H_{cm})	0.500	0.333	0.500	0.535	0.667	0.563

$CN(Ca^{2+}/CO_3^{2-}) = CN(CO_3^{2-}/Ca^{2+}) = 8$. In monohydrocalcite, $CN(Ca^{2+}) = CN(CO_3^{2-}) = 6$, $CN(H_2O) = 4$; the structure contains an unclassified 3-transitive 4,6-coordinated net with the $(4^2.5^4)(4^6.5^6.6^2.7)_2$ point symbol. Thus, all symmetrically independent Ca^{2+} cations and CO_3^{2-} groups in this net, as well as all water molecules, have topologically similar environments. In ikaite $CN(Ca^{2+}) = 7$, $CN(CO_3^{2-}) = 9$); two water molecules have CN = 4 and one molecule has CN = 3. The net of contacts in this case is 5-transitive; the point symbol is $(4.5^2)_2(4^2.5^3.6)_2(4^3.5^{10}.6^7.8)(4^3.5^3)_2(4^5.5^{12}.6^7.7^8.8^4)$, where vertices with the subscript 2 correspond to the centers of mass of water molecules, $4^3.5^{10}.6^7.8$ corresponds to Ca^{2+} ions; $4^5.5^{12}.6^7.7^8.8^4$ corresponds to carbonate ions.

Fig. 3 shows the number of symmetrically independent edges of the net e'' as a decreasing function of the minimal solid angle (minΩ) for the removal of contacts. The circles show the e'' values in the critical net. According to (10), $e''_{crit} = \inf(e''_{crit})$ in all structures, except for ikaite. In the ikaite structure, this number is one unity larger than the infimum. The results of statistical analysis in molecular crystals showed [51] that the distribution of a random variable $(e''_{crit} - \inf(e''_{crit}))$ is similar to the branch of the normal discrete distribution with $\mu = 0$, i.e. $(e''_{crit} - \inf(e''_{crit})) \le 2$ for more than 90% of molecular structures. Apparently, this regularity is true also for the nets of contacts in nonmolecular crystals. The range of Ω values increases in the calcite–postaragonite–aragonite–monohydrocalcite–vaterite–ikaite row and indicates that the homogeneity of the Delone system of the centers of mass of structural units decreases in this row. Since the CN value for postaragonite is larger than those of calcite, aragonite, and vaterite, the range of Ω values ends at the critical value of calcite and vaterite (with an accuracy up to half integer $\Omega_{crit} = 16.5\%$). The average value Ω over all contacts always decreases with increasing average CN value over all structural units: $\langle\Omega\rangle = 100\%/\langle CN\rangle$. We have $\langle\Omega\rangle = 100/6 = 16.67\%$ for calcite, aragonite, and vaterite, $\langle\Omega\rangle = 100/8 = 12.50\%$ for postaragonite, $\langle\Omega\rangle = 100/5.33 = 18.75\%$ for monohydrocalcite, and $\langle\Omega\rangle = 100/4.75 = 21.05\%$ for ikaite. However, Ω_{crit} may differ from the average value: the $\Omega_{crit} - \langle\Omega\rangle$ difference is equal to 0 for calcite and vaterite (for vaterite this equality is approximate), slightly smaller than zero for monohydrocalcite, aragonite, and postaragonite, and significantly smaller than zero for ikaite. That is why seemingly insignificant contacts $CO_3^{2-}\ldots H_2O$ ($\Omega_{crit} = 11.9\%$) in ikaite are classified as structure-forming ones.

The calcite structural class $R\bar{3}c$, $Z = 6(\bar{3}; 32)$ belongs to the classes where only one base contact is possible (see our publications in JSC, 2022), even though this class has never been found in molecular crystals [52]. Indeed, the calcite structure has only one symmetrically unique contact; therefore, the critical net in the calcite structure coincides with the

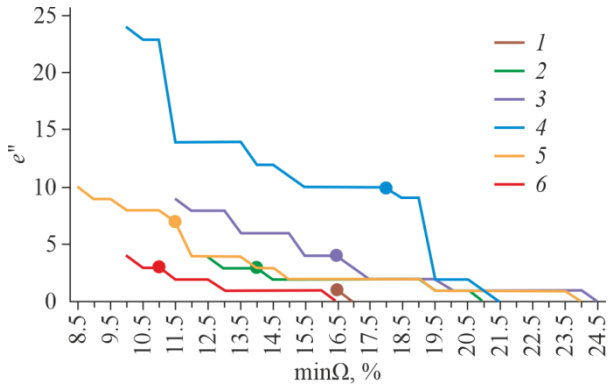

Fig. 3. Number of symmetrically independent contacts between the crystal's structural units e'' as a function of the minimal solid angle (minΩ) for the removal of contacts with a step of 0.5% for calcite (*1*), aragonite (*2*), vaterite (*3*), monohydrocalcite (*4*), ikaite (*5*), post-aragonite (*6*). The circles show the e''_{crit} values.

original net of **pcu** contacts. The critical net in the postaragonite structure belongs to the same type, but has three unique contacts.

In the aragonite structure, we have $e''_{crit} = 3$, $CN_{crit}(Ca^{2+}) = CN_{crit}(CO_3^{2-}) = 4$; the critical net, in contrast to the original net of contacts, is vertex-transitive in the idealized version and belongs to the **sra** type ($SrAl_2$, Fig. 4*a*). A net of this type (along with **gsi** (γ-Si), **crb** (CrB_4), and **gis** (natural zeolite gismondine)) is formed in tetrahedral and disphenoidal coordination environments of structural units in the 1:1 ratio [53]. In the critical net of aragonite, the centers of mass of CO_3^{2-} groups have a distorted disphenoidal environment, and Ca^{2+} cations have a distorted tetrahedral environment.

Table 2 lists the coordination numbers in the critical net of the vaterite structure $e''_{crit} = 4$. In one of symmetrically independent pairs, the ions denoted $Ca^{2+(2)}$ and $CO_3^{2-(1)}$ have CN = 2. Strictly speaking, a vertex degree cannot be less than three in a crystallographic net; therefore, one- and two-coordinated vertices are to be removed from net classifications [54]. Then the only remaining vertices are four-coordinated vertices corresponding to $Ca^{2+(1)}$ with a distorted square coordination and to $CO_3^{2-(2)}$ with a distorted tetrahedral coordination, and this net belongs to the **pts** topological type (PtS, Fig. 4*b*).

In the monohydrocalcite structure, $e''_{crit} = 10$, which is the largest value among all of the considered structures, despite the fact that the $P3_1$ space group has the smallest value $|U_{SG}| = 2$. The reason is that the $P3_1$ group has no stationary orbits, whence it follows that $|U_{PG}| = 0$. Therefore, according to (10), $\inf(e''_{crit}) = 2 + 9 - 1 - 0 = 10$ in the monohydrocalcite structure. The coordination numbers for the critical net are listed in Table 3. After removing one- and two-coordinated vertices (all Ca^{2+} cations and the centers of mass of all water molecules), the net adopts the **qtz** topological type (quartz, Fig. 4*c*). The centers of mass are located in the net $CO_3^{2-(3)}$ vertices, while the centers of mass of $CO_3^{2-(1)}$ and $CO_3^{2-(2)}$ are removed together with Ca^{2+} and water molecules, since they become two-coordinated after the latter are removed. Note that both **qtz** and **pts** become edge-transitive in the idealized version.

In the ikaite structure, we have $e''_{crit} = 7$, which is, as already mentioned, only one unit larger than $\inf(e''_{crit})$. In this case, the contact between Ca^{2+} and CO_3^{2-} located on the same second-order rotation axis (Wyckoff position 4*e*) is redundant

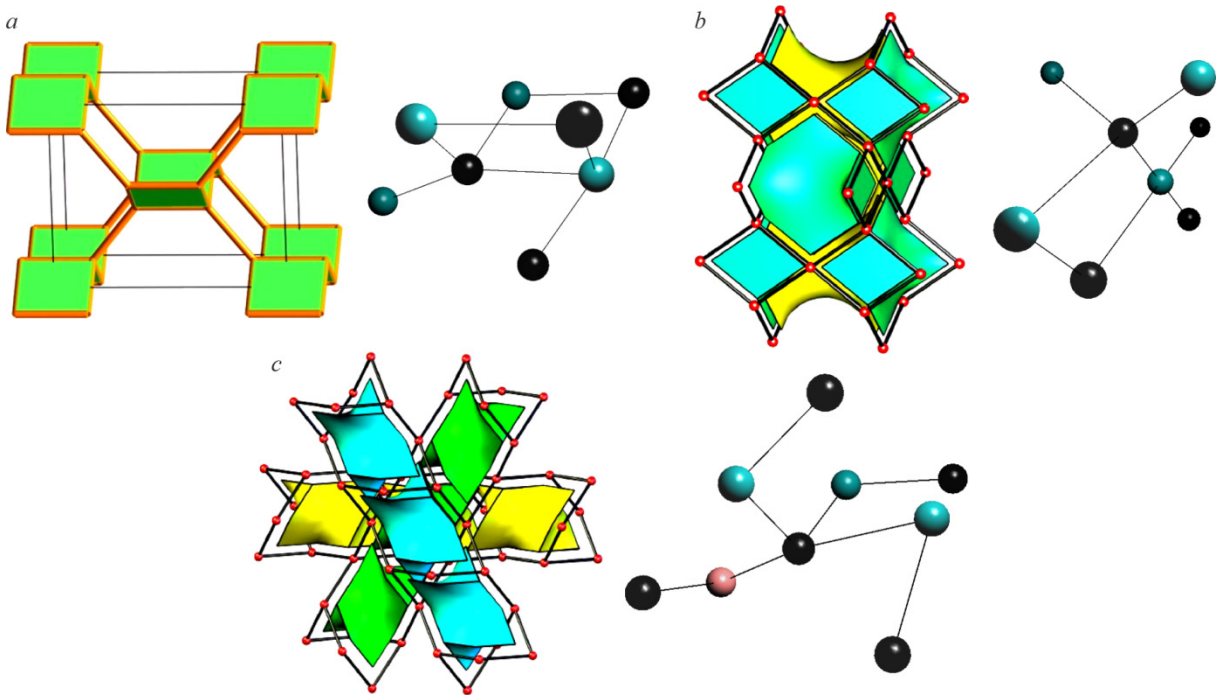

Fig. 4. Topological types **sra** (*a*), **pts** (*b*), and **qtz** (*c*) in RCSR [44] (left), coordination environment of vertices in the critical nets of aragonite (*a*), vaterite (*b*), and monohydrocalcite (*c*) (right).

TABLE 2. Coordination Numbers CN(*X*/*Y*) in the Crystal Structure and in the Vaterite Critical Net (in parentheses)

X	*Y*				CN_Σ
	$Ca^{2+\,(1)}$	$Ca^{2+\,(2)}$	$CO_3^{2-\,(1)}$	$CO_3^{2-\,(2)}$	
$Ca^{2+\,(1)}$	0	0	4(2)	2(2)	6(4)
$Ca^{2+\,(2)}$	0	0	4(1)	2(1)	6(2)
$CO_3^{2-\,(1)}$	2(1)	4(1)	0	0	6(2)
$CO_3^{2-\,(2)}$	2(2)	4(2)	0	0	6(4)

TABLE 3. Coordination Numbers CN(*X*/*Y*) in the Crystal Structure and in the Monohydrocalcite Net of Base Contacts (in parentheses)

X	*Y*									CN_Σ
	$Ca^{2+\,(1)}$	$Ca^{2+\,(2)}$	$Ca^{2+\,(3)}$	$CO_3^{2-\,(1)}$	$CO_3^{2-\,(2)}$	$CO_3^{2-\,(3)}$	$H_2O^{(1)}$	$H_2O^{(2)}$	$H_2O^{(3)}$	
$Ca^{2+\,(1)}$	0	0	0	1(1)	0	3(1)	0	2(0)	0	6(2)
$Ca^{2+\,(2)}$	0	0	0	0	3(1)	1(1)	2(0)	0	0	6(2)
$Ca^{2+\,(3)}$	0	0	0	3(1)	1(1)	0	0	0	2(0)	6(2)
$CO_3^{2-\,(1)}$	1(1)	0	3(1)	0	0	0	2(1)	0	0	6(3)
$CO_3^{2-\,(2)}$	0	3(1)	1(1)	0	0	0	0	2(1)	0	6(3)
$CO_3^{2-\,(3)}$	3(1)	1(1)	0	0	0	0	0	0	2(1)	6(4)
$H_2O^{(1)}$	0	2(0)	0		0	0	0	0	0	4(1)
$H_2O^{(2)}$	2(0)	0	0	0		0	0	0	0	4(1)
$H_2O^{(3)}$	0	0	2(0)	0	0	2(2)	0	0	0	4(2)

for the generating set. Through this contact, the carbonate anion chelates the Ca^{2+} cation whose first coordination sphere was considered to be the fundamental building unit (FBU) of the ikaite structure [3]. The coordination numbers in this structure are listed in Table 4.

Interestingly, one of $H_2O^{(1)}$ water molecules in the ikaite critical net maintains all its contacts from the original net, and the CN does not decrease. After the two-coordinated vertices (centers of mass of $H_2O^{(2)}$) are removed from the critical net, it is no longer classified by known databases. All water ions and molecules have different coordination environments, and the difference between environments appears only beginning with the fourth coordination sphere for Ca^{2+} and CO_3^{2-}, and from the fifth coordination sphere for water molecules (Table 5).

TABLE 4. Coordination Numbers CN(*X*/*Y*) in the Crystal Structure and in the Ikaite Critical Net (in parentheses)

X	*Y*					CN_Σ
	Ca^{2+}	CO_3^{2-}	$H_2O^{(1)}$	$H_2O^{(2)}$	$H_2O^{(3)}$	
Ca^{2+}	0	1(1)	2(2)	2(2)	2(0)	7(5)
CO_3^{2-}	1(1)	0	2(2)	2(0)	4(2)	9(5)
$H_2O^{(1)}$	1(1)	1(1)	0	1(1)	0	3(3)
$H_2O^{(2)}$	1(0)	1(0)	1(1)	0	1(1)	4(2)
$H_2O^{(3)}$	1(1)	2(1)	0	1(1)	0	4(3)

TABLE 5. First 10 Coordination Spheres of H_2O Molecules in the Simplified Critical Net of Ikaite

No.	1st	2d	3d	4th	5th	6th	7th	8th	9th	10th
Ca^{2+}	5	12	25	46	71	96	137	180	221	274
CO_3^{2-}	5	12	25	42	71	104	135	172	223	278
$H_2O^{(1)}$	3	10	24	43	67	100	134	174	222	275
$H_2O^{(3)}$	3	10	24	43	66	96	133	176	221	271

If all edges are removed from the original net of contacts in the ikaite structure, then all possible nets obtained by adding no more than $\inf(e''_{crit}) = 6$ symmetrically independent edges constitute a total of 847 combinatorially distinct variants. Only 166 of them have 3D nets; one variant out of 166 has a 3D net and island graphs; and 36 variants have 0-coordinated vertices. Without these variants, 129 combinatorially different nets remain, but 25 of them have two interpenetrating nets, i.e. the net is not simply connected. Thus, there are 104 possible combinatorially different critical nets in the ikaite structural class. After removing 1- and 2-coordinated vertices, the remaining nets include ten 5-coordinated nets of the **bnn** topological type ("single-layer graphite" BN, Fig. 5*a*), five 3.6-coordinated nets of the **ant** topological type (anatase, Fig. 5*b*), one 6-coordinated **pcu**, one 3.5-coordinated **gra** (bilayer graphite, Fig. 5*c*), one 4-coordinated **gis** (gismondin, Fig. 5*d*), and other nets. Thus, different critical coordination numbers are possible for the same e''_{crit}. The **bnn** and **pcu** types are the most common critical nets in molecular crystals with the corresponding CN_{crit} [51].

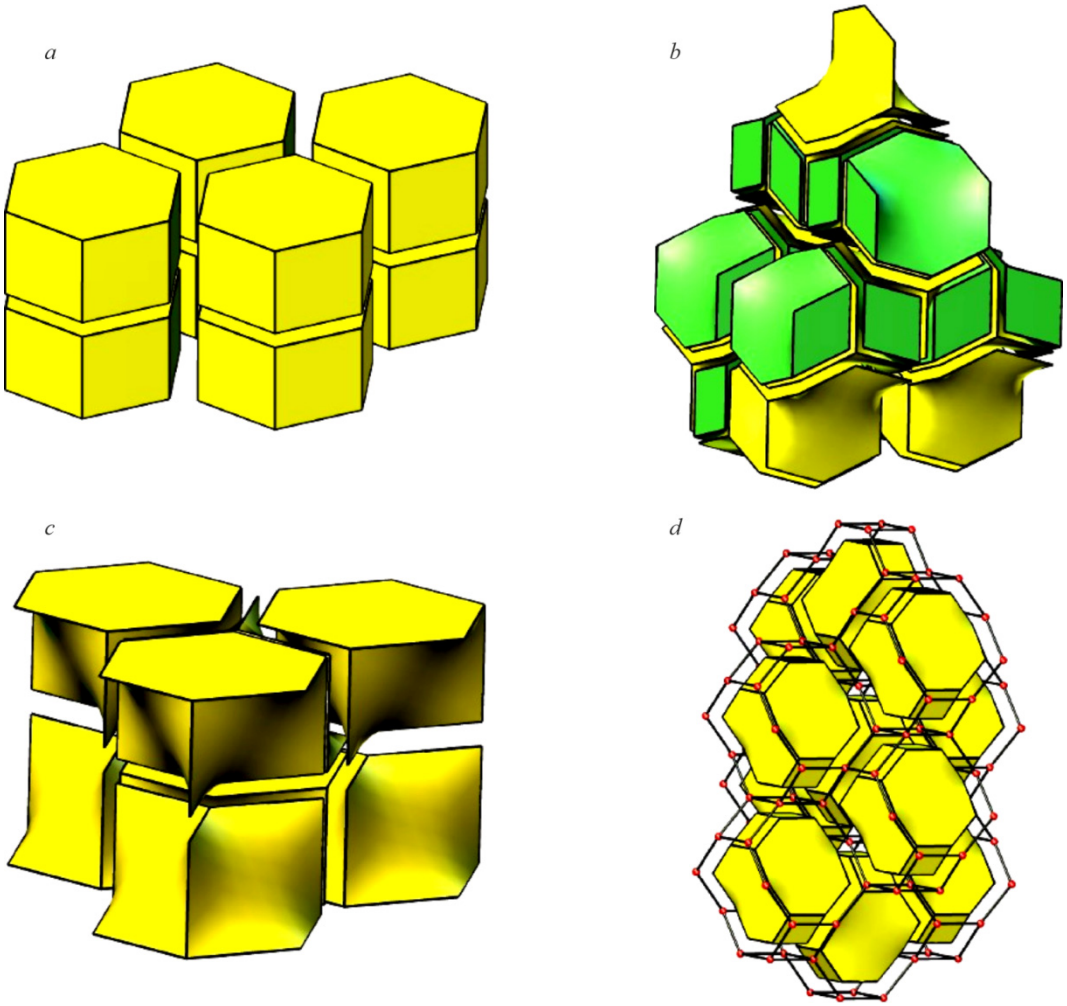

Fig. 5. Topological types **bnn** (*a*), **ant** (*b*), **gra** (*c*), and **gis** (*d*) in RCSR [44].

All 104 possible critical nets can be divided into two groups. The first one contains a generating set of contacts with exactly one symmetrically independent involution (contact of order 1 relative to the center of inversion); therefore, $e = 22$ (56 nets). The second group has no involutions in the generating set; therefore, $e = 24$ (48 nets). The H_{edge} values in the first and second groups are 2.550 bit/contact and 2.585 bit/contact, respectively. In the real ikaite structure, this value is slightly larger (2.777 bit/contact) due to the presence of a redundant contact in the generating set (Table 6). The only contact of order 1 is the redundant contact of Ca^{2+} and CO_3^{2-} occupying the 4*e* position (see above).

According to the rule of strong additivity, information complexity can be expressed in terms of individual contributions from several sources of information [55, 56]. In a crystal, such possible sources are symmetrically independent structural units. Let value $H_{CN,i}$ (bit/ structural unit) characterize the complexity of the first coordination sphere of the *i*th structural unit:

$$H_{\mathrm{CN},i} = -\sum_j \frac{\mathrm{CN}_j}{\mathrm{CN}_i} \log_2 \frac{\mathrm{CN}_j}{\mathrm{CN}_i}, \tag{12}$$

where CN_i is the coordination number of the *i*th structural unit; CN_j is the number of symmetrically equivalent contacts of the *j*th type in the coordination sphere of the *i*th structural unit. Then the total complexity of first coordination spheres in the crystal is

$$H_{\mathrm{CN}} = \sum_{i=1}^{v''} \frac{v_j}{v} \cdot H_{\mathrm{CN},i} + H(\mathrm{CN}_1, \mathrm{CN}_2, \ldots, \mathrm{CN}_v) \tag{13}$$

where, in view of (7):

$$H(\mathrm{CN}_1, \mathrm{CN}_2, \ldots, \mathrm{CN}_v) = -\sum_{i=1}^{v''} v_i \cdot \frac{\mathrm{CN}_i}{2e} \log_2 \frac{\mathrm{CN}_i}{2e}. \tag{14}$$

However, H_{CN} does not coincide with H_{edge}, since the second quantity does not take into account the partitioning of symmetrically nonequivalent contacts over coordination spheres of different structural units:

$$H_{\mathrm{CN}} = H_{\mathrm{edge}} + \Delta H_{\mathrm{edge}}, \tag{15}$$

TABLE 6. Structural Data and Information Complexity of the Net of Contacts in the $CaCO_3$ Polymorphs

Structural data		Calcite	Aragonite	Postaragonite	Vaterite	Monohydrocalcite	Ikaite
Net	Topological type	**pcu**	**nia**	**bcu**	**nia**	$(4^2.5^4)(4^6.5^6.6^2.7)_2$	$(4.5^2)_2(4^2.5^3.6)_2$ $(4^3.5^{10}.6^7.8)(4^3.5^3)_2$ $(4^5.5^{12}.6^7.7^8.8^4)$
	e	12	24	16	36	72	38
	e″	1	4	4	9	24	10
	WP	*f*	d^2c^2	f^2e^2	f^9	a^{24}	f^9e
	H_{edge}, bit/contact	0	1.918	2.000	3.170	4.585	3.301
	SIC(H_{edge})	0	0.418	0.500	0.613	0.743	0.629
Critical net	Topological type	**pcu**	**sra**	**pcu**	**pts**	**qtz**	$(6^3)_2(6^7.8^2.10)$
	e	12	16	12	16	30	26
	inf *e*″	1	3	3	4	10	6
	e″	1	3	3	4	10	7
	WP	*f*	dc^2	fe^2	f^4	a^{10}	f^6e
	$H_{edge, crit}$, bit/contact	0	1.500	1.585	2.000	3.322	2.777
	SIC(H_{edge})	0	0.375	0.442	0.500	0.677	0.591

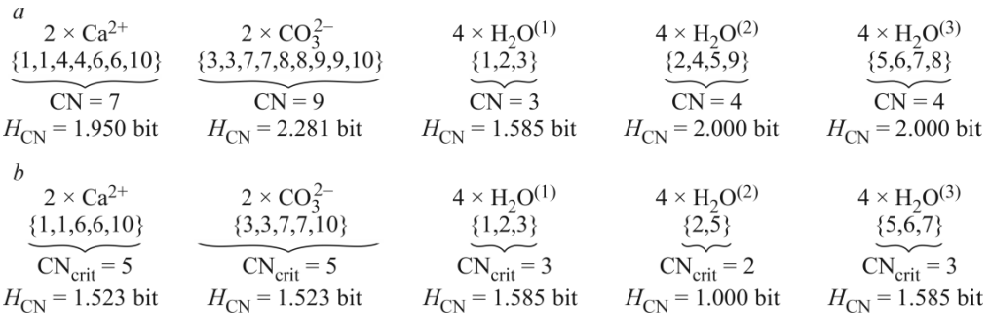

Fig. 6. Information complexity of coordination spheres of ikaite structural units ($v = 16$) in the net of all contacts (*a*) and in the critical net (*b*). Numbers denote symmetrically equivalent contacts.

where ΔH_{edge} characterizes the increase of information content due to the distribution of symmetrically unique contacts over structural units of the crystal.

For example, the reduced unit cell of ikaite contains 16 centers of mass, and five of them are symmetrically unique (Fig. 6*a*). For water molecules, $H_{CN}(H_2O^{(1)}) = -3 \cdot 1/3 \cdot \log_2(1/3) = 1.585$ bit, $H_{CN}(H_2O^{(2)}) = H_{CN}(H_2O^{(3)}) = -4 \cdot 1/4 \cdot \log_2(1/4) = 2.000$ bit. Similarly, $H_{CN}(Ca^{2+}) = -3 \cdot 2/7 \cdot \log_2(2/7) - 1/7 \cdot \log_2(1/7) = 1.950$ bit, $H_{CN}(CO_3^{2-}) = -4 \cdot 2/9 \cdot \log_2(2/9) - 1/9 \cdot \log_2(1/9) = 2.281$ bit. Therefore, $\sum_{i=1}^{v''} \frac{v_j}{v} \cdot H_{CN,i} = 4/16 \cdot (1.585 + 2.000 + 2.000) + 2/16 \cdot (1.950 + 2.281) = 1.925$ bit. Also, $H(CN_1, CN_2, \ldots CN_{16}) = H(2\times\{7\}, 2\times\{9\}, 4\times\{3\}, 8\times\{4\}) = 3.888$ bit. Therefore, $H_{CN} = 1.925 + 3.888 = 5.813$ bit. As can be seen from Table 6, $H_{edge} = 3.301$ bit; therefore, it follows from (15) that $\Delta H_{edge} = 5.813 - 3.301 = 2.512$ bit.

Fig. 6*b* shows the H_{CN} values of ikaite structural units for the critical net. The sum $\sum_{i=1}^{v''} \frac{v_j}{v} \cdot H_{CN,i}$ is equal to 1.423 bit. Then we have $H(CN_1, CN_2, \ldots CN_{16}) = H(4\times\{5\}, 4\times\{2\}, 8\times\{3\}) = 3.922$ bit, i.e. even a little larger than in the original net of contacts. Therefore, the total value $H_{CN} = 1.423 + 3.922 = 5.345$ bit. As can be seen from Table 6, $H_{edge} = 2.777$ bit; therefore, according to (15), $\Delta H_{edge} = 5.345 - 2.777 = 2.568$ bit, i.e. only 0.056 bit larger than the corresponding value for the original net of contacts. Correlations between H_{CN}, $H(CN_1, CN_2, \ldots CN_v)$ and H_{edge} can be further investigated using a large sample of crystal structures.

CONCLUSIONS

Calcium carbonate polymorphs and crystalline hydrates of calcium carbonate were analyzed topologically and the numbers of generating contacts in their crystal structures were determined for the first time.

FUNDING

This work was partially funded by the Russian Science Foundation, grant No. 20-77-10065 (topological analysis).

The information indices were calculated by D. A. Banaru within the State Assignment for Vernadsky Institute of Geochemistry and Analytical Chemistry of RAS.

CONFLICT OF INTERESTS

The authors declare that they have no conflicts of interests.

REFERENCES

1. L. N. Kogarko. *Geochem. Int.*, **2006**, *44*, 3. https://doi.org/10.1134/S0016702906010022
2. È. P. Solotchina and P. A. Solotchin. *J. Struct. Chem.*, **2014**, *55*, 779. https://doi.org/10.1134/S0022476614040295
3. N. Tateno and A. Kyono. *J. Mineral. Petrol. Sci.*, **2014**, *109*, 157. https://doi.org/10.2465/jmps.140320
4. P. N. Gavryushkin, A. B. Belonoshko, N. Sagatov, D. Sagatova, E. Zhitova, M. G. Krzhizhanovskaya, A. Rečnik, E. V. Alexandrov, I. V. Medrish, Z. I. Popov, and K. D. Litasov. *Cryst. Growth Des.*, **2021**, *21*, 65. https://doi.org/10.1021/acs.cgd.0c00589
5. B. Pokroy, J. S. Fieramosca, R. B. Von Dreele, A. N. Fitch, E. N. Caspi, and E. Zolotoyabko. *Chem. Mater.*, **2007**, *19*, 3244. https://doi.org/10.1021/cm070187u
6. A. G. Christy. *Cryst. Growth Des.*, **2017**, *17*, 3567. https://doi.org/10.1021/acs.cgd.7b00481
7. A. A. Krylov, E. A. Logvina, T. V. Matveeva, E. M. Prasolov, V. F. Sapega, A. L. Demidova, and M. S. Radchenko. *Zap. Ross. Mineral. O-va*, **2015**, *144*, 61. [In Russian]
8. S. Ono, T. Kikegawa, Y. Ohishi, and J. Tsuchiya. *Am. Mineral.*, **2005**, *90*, 667. https://doi.org/10.2138/am.2005.1610
9. A. R. Oganov, C. W. Glass, and S. Ono. *Earth Planet. Sci. Lett.*, **2006**, *241*, 95. https://doi.org/10.1016/j.epsl.2005.10.014
10. M. Merlini, M. Hanfland, and W. A. Crichton. *Earth Planet. Sci. Lett.*, **2012**, *333*/*334*, 265. https://doi.org/10.1016/j.epsl.2012.04.036
11. P. N. Gavryushkin, N. S. Martirosyan, T. M. Inerbaev, Z. I. Popov, S. V. Rashchenko, A. Yu. Likhacheva, S. S. Lobanov, A. F. Goncharov, V. B. Prakapenka, and K. D. Litasov. *Cryst. Growth Des.*, **2017**, *17*, 6291. https://doi.org/10.1021/acs.cgd.7b00977
12. P. N. Gavryushkin, N. Sagatov, A. B. Belonoshko, M. V. Banaev, and K. D. Litasov. *J. Phys. Chem. C*, **2020**, *124*, 26467. https://doi.org/10.1021/acs.jpcc.0c08309
13. D. Sagatova, A. Shatskiy, N. Sagatov, P. N. Gavryushkin, and K. D. Litasov. *Lithos*, **2020**, *370*/*371*, 105637. https://doi.org/10.1016/j.lithos.2020.105637
14. D. N. Sagatova, A. F. Shatskiy, P. N. Gavryushkin, N. E. Sagatov, and K. D. Litasov. *ACS Earth Space Chem.*, **2021**, *5*, 1709. https://doi.org/10.1021/acsearthspacechem.1c00065
15. S. V. Borisov, S. A. Magarill, and N. V. Pervukhina. *Crystallogr. Rep.*, **2011**, *56*, 935. https://doi.org/10.1134/S1063774511060046
16. S. V. Borisov, S. A. Magarill, and N. V. Pervukhina. *J. Struct. Chem.*, **2012**, *53*, 55. https://doi.org/10.1134/S0022476612070086
17. S. V. Borisov, N. V. Pervukhina, and S. A. Magarill. *Struct. Chem.*, **2016**, *27*, 1673. https://doi.org/10.1007/s11224-016-0799-5
18. S. V. Borisov, S. A. Magarill, and N. V. Pervukhina. *Russ. Chem. Rev.*, **2015**, *84*, 393. https://doi.org/10.1070/RCR4479
19. S. V. Borisov, S. A. Magarill, and N. V. Pervukhina. *Crystallogr. Rep.*, **2019**, *64*, 30. https://doi.org/10.1134/S1063774519010036
20. Ya. O. Shablovsky. *Mineralogy*, **2019**, *5*(3), 3. https://doi.org/10.35597/2313-545X-2019-5-3-3-10
21. Ya. O. Shablovsky. *Mineralogy*, **2019**, *5*(2), 3. https://doi.org/10.35597/2313-545X-2019-5-2-3-9
22. S. V. Krivovichev. *Acta Crystallogr*., *Sect. B: Struct. Sci.*, **2016**, *72*, 274. https://doi.org/10.1107/s205252061501906x
23. S. Krivovichev. *Acta Crystallogr*., *Sect. A: Found. Adv.*, **2012**, *68*, 393. https://doi.org/10.1107/S0108767312012044
24. D. S. Sabirov and I. S. Shepelevich. *Entropy*, **2021**, *23*, 1240. https://doi.org/10.3390/e23101240
25. E. A. Lord and A. M. Banaru. *Moscow Univ. Chem. Bull.*, **2012**, *67*, 50. https://doi.org/10.3103/S0027131412020034
26. A. M. Banaru and V. R. Shiroky. *Crystallogr. Rep.*, **2019**, *64*, 201. https://doi.org/10.1134/S1063774519020044
27. A. M. Banaru and V. R. Shiroky. *Crystallogr. Rep.*, **2020**, *65*, 417. https://doi.org/10.1134/S1063774520030050
28. A. M. Banaru. *Moscow Univ. Chem. Bull.*, **2019**, *74*, 101. https://doi.org/10.3103/S0027131419030039

29. A. M. Banaru, V. R. Shiroky, and D. A. Banaru. *Crystallogr. Rep.*, **2021**, *66*, 913. https://doi.org/10.1134/S1063774521060043
30. N. Dolbilin. *Struct. Chem.*, **2016**, *27*, 1725. https://doi.org/10.1007/s11224-016-0832-8
31. I. A. Baburin, M. Bouniaev, N. Dolbilin, N. Yu. Erokhovets, A. Garber, S. V. Krivovichev, and E. Schulte. *Acta Crystallogr*., *Sect. A: Found. Adv.*, **2018**, *74*, 616. https://doi.org/10.1107/s2053273318012135
32. V. A. Blatov. *Crystallogr. Rev.*, **2004**, *10*, 249. https://doi.org/10.1080/08893110412331323170
33. V. A. Blatov. *J. Struct. Chem.*, **2009**, *50*, 160. https://doi.org/10.1007/s10947-009-0204-y
34. M. W. Anderson, J. T. Gebbie-Rayet, A. R. Hill, N. Farida, M. P. Attfield, P. Cubillas, V. A. Blatov, D. M. Proserpio, D. Akporiaye, B. Arstad, and J. D. Gale. *Nature*, **2017**, *544*, 456. https://doi.org/10.1038/nature21684
35. V. A. Blatov and Y. A. Zakutkin. *Z. Kristallogr. – Cryst. Mater.*, **2002**, *217*, 464. https://doi.org/doi:10.1524/zkri.217.9.464.22882
36. A. Banaru and A. Kochnev. *Stud. Univ. Babes-Bolyai*, *Chem.*, **2017**, *62*, 121. https://doi.org/10.24193/subbchem.2017.1.10
37. A. M. Banaru and D. M. Gridin. *Moscow Univ. Chem. Bull.*, **2019**, *74*, 265. https://doi.org/10.3103/S0027131419060051
38. D. M. Gridin and A. M. Banaru. *Moscow Univ. Chem. Bull.*, **2020**, *75*, 354. https://doi.org/10.3103/S0027131420060115
39. J. P. R. De Villiers. *Am. Mineral.*, **1971**, *56*, 758.
40. E. Mugnaioli, I. Andrusenko, T. Schüler, N. Loges, R. E. Dinnebier, M. Panthöfer, W. Tremel, and U. Kolb. *Angew. Chem. Int. Ed.*, **2012**, *51*, 7041. https://doi.org/10.1002/anie.201200845
41. S. Gražulis, A. Daškevič, A. Merkys, D. Chateigner, L. Lutterotti, M. Quirós, N. R. Serebryanaya, P. Moeck, R. T. Downs, and A. Le Bail. *Nucleic Acids Res.*, **2012**, *40*, D420. https://doi.org/10.1093/nar/gkr900
42. R. T. Downs and M. Hall-Wallace. *Am. Mineral.*, **2003**, *88*, 247.
43. V. A. Blatov, A. P. Shevchenko, and D. M. Proserpio. *Cryst. Growth Des.*, **2014**, *14*, 3576. https://doi.org/10.1021/cg500498k
44. M. O′Keeffe, M. A. Peskov, S. J. Ramsden, and O. M. Yaghi. *Acc. Chem. Res.*, **2008**, *41*, 1782. https://doi.org/10.1021/ar800124u
45. Topcryst: The Samara Topological Data Center. https://topcryst.com
46. V. A. Blatov, M. O′Keeffe, and D. M. Proserpio. *CrystEngComm*, **2010**, *12*, 44. https://doi.org/10.1039/b910671e
47. V. A. Blatov, A. P. Shevchenko, and V. N. Serenzhkin. *Acta Crystallogr*., *Sect. A*, **1995**, *51*, 909. https://doi.org/10.1107/S0108767395006799
48. A. M. Banaru, S. M. Aksenov, and S. V. Krivovichev. *Symmetry*, **2021**, *13*, 1399.
49. A. M. Banaru. *Crystallogr. Rep.*, **2018**, *63*, 1077. https://doi.org/10.1134/S1063774518070052
50. W. F. Kolbe and A. Smakula. *Phys. Rev.*, **1961**, *124*, 1754. https://doi.org/10.1103/PhysRev.124.1754
51. A. M. Banaru, S. M. Aksenov, and D. A. Banaru. *Moscow Univ. Chem. Bull.*, **2021**, *76*, 325. https://doi.org/10.3103/S0027131421050023
52. V. K. Belsky, O. N. Zorkaya, and P. M. Zorky. *Acta Crystallogr*., *Sect. A*, **1995**, *51*, 473. https://doi.org/10.1107/S0108767394013140
53. V. A. Blatov and D. M. Proserpio. Periodic-Graph Approaches in Crystal Structure Prediction. In: Modern Methods of Crystal Structure Prediction / Ed. A.R. Oganov. Wiley-VCH, **2010**, 1-28. https://doi.org/10.1002/9783527632831.ch1
54. J. G. Eon. *Acta Crystallogr*., *Sect. A: Found. Adv.*, **2016**, *72*, 376. https://doi.org/10.1107/S2053273316003867
55. W. Hornfeck. *Acta Crystallogr*., *Sect. A: Found. Adv.*, **2020**, *76*, 534. https://doi.org/10.1107/S2053273320006634a
56. W. Hornfeck. *Z. Kristallogr. – Cryst. Mater.*, **2022**. https://doi.org/doi:10.1515/zkri-2021-2062